Available online at www.sciencedirect.com
ScienceDirect
Deep-Sea Research II 54 (2007) 2543–2559
DEEP-SEA RESEARCH PART II
www.elsevier.com/locate/dsr2

Comparison of atmospheric forcing in four sub-arctic seas

Muyin Wang[a,*], Nicholas A. Bond[a], James E. Overland[b]

[a]Joint Institute for Study of Atmosphere and Ocean, Box 354235, University of Washington, Seattle, Washington 98195, USA
[b]Pacific Marine Environmental Laboratory, National Ocean and Atmosphere Administration, 7600 Sand Point Way NE, Seattle, Washington 98115, USA

Received in revised form 9 August 2007; accepted 21 August 2007
Available online 22 October 2007

Abstract

A comparative analysis was conducted on climate variability in four sub-arctic seas: the Sea of Okhotsk, the Bering Sea shelf, the Labrador Sea, and the Barents Sea. Based on data from the NCEP/NCAR reanalysis, the focus was on air–sea interactions, which influence ice cover, ocean currents, mixing, and stratification on sub-seasonal to decadal time scales. The seasonal cycles of the area-weighted averages of sea-level pressure (SLP), surface air temperature (SAT) and heat fluxes show remarkable similarity among the four sub-arctic seas. With respect to variation in climate, all four seas experience changes of comparable magnitude on interannual to interdecadal time scales, but with different timing. Since 2000 warm SAT anomalies were found during most of the year in three of the four sub-arctic seas, with the exception of the Sea of Okhotsk. A seesaw (out of phase) pattern in winter SAT anomalies between the Labrador and the Barents Sea in the Atlantic sector is observed during the past 50 years before 2000; a similar type of co-variability between the Sea of Okhotsk and the Bering Sea shelf in the Pacific is only evident since 1970s. Recent positive anomalies of net heat flux are more prominent in winter and spring in the Pacific sectors, and in summer in the Atlantic sectors. There is a reduced magnitude in wind mixing in the Sea of Okhotsk since 1980, in the Barents Sea since 2000, and in early spring/late winter in the Bering Sea shelf since 1995. Reduced sea-ice areas are seen over three out of four (except the Sea of Okhotsk) sub-arctic seas in recent decades, particularly after 2000 based on combined in situ and satellite observations (HadISST). This analysis provides context for the pan-regional synthesis of the linkages between climate and marine ecosystems.

Keywords: Atmospheric forcing; Surface heat fluxes; Sea of Okhotsk (44–62°N; 135–160°E); Bering Sea shelf (52–66°N; 180–150°W); Labrador Sea (46–69°N; 66–43°W); Barents Sea (66–81°N; 14–66°E)

1. Introduction

The four major sub-arctic seas, the Sea of Okhotsk, the Bering Sea (eastern shelf), the Labrador Sea, and the Barents Sea (Fig. 1), support extraordinarily rich marine resources, which provide food and wealth to regional economies and local communities. These sub-arctic seas share several common features: seasonal ice cover, freshwater sources from ice-melt and runoff, pronounced seasonality in winds and surface heat fluxes, high ecosystem abundance, and low biodiversity (Hunt and Drinkwater, 2005). Having similar sub-arctic locations, they represent transition zones between the influences of cold, dry air masses of arctic or continental origin and maritime air masses originating

*Corresponding author. Tel.: +1 206 526 4532; fax: +1 206 526 6485.
E-mail address: muyin.wang@noaa.gov (M. Wang).

0967-0645/$ - see front matter © 2007 Elsevier Ltd. All rights reserved.
doi:10.1016/j.dsr2.2007.08.014

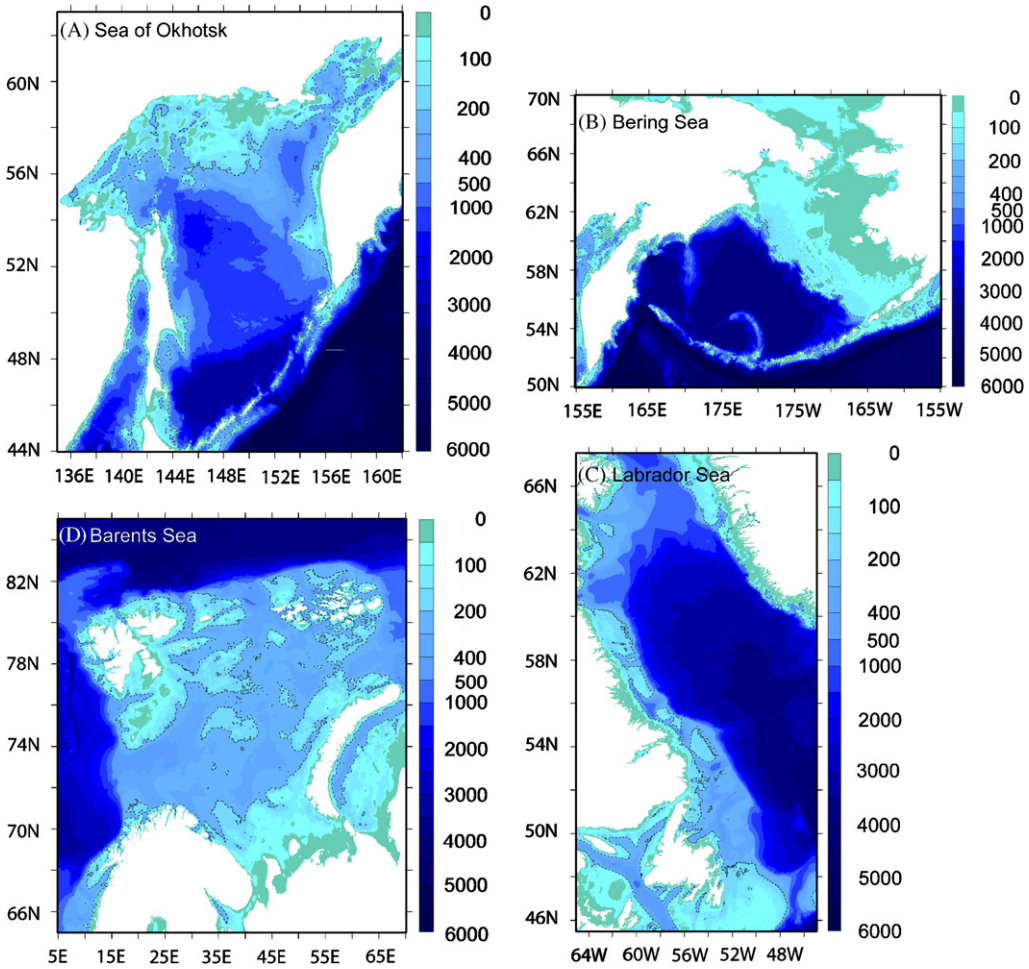

Fig. 1. The bathymetry of the sub-arctic seas based on high resolution topography data ETOPO2.

over the open oceans to the south. Their atmospheric climates differ to some extent in the mean, and to a substantial degree in terms of the variability. In turn, these variations modulate ocean currents, heating, mixing and the exchange of water with neighboring basins.

The importance of climate-induced changes to the productivity and community structure of high-latitude marine ecosystems has become increasingly appreciated (e.g., Ottersen et al., 2000; Hunt and Megrey, 2005). A key aspect of the ecosystems of these four sub-arctic seas is their commercial fisheries. The yields from these fisheries depend in part on ocean productivity, water temperatures and ocean currents. Among a host of factors, these ecosystems appear to be particularly sensitive to the extent and timing of sea ice in winter and spring, and upper-ocean stratification during summer (Drinkwater, 2002; Hunt et al., 2002; Baier and Napp, 2003; Ottersen et al., 2004). Yet these parameters are closely related to changes in atmospheric climatic conditions. The present study presents a comparison of the means and variability of the climate of the four sub-arctic seas, emphasizing parameters relevant to air–sea interactions.

Most previous studies of the climate and air–sea interactions over the four sub-arctic seas are regional specific. For example, Liu et al. (2007) and Sasaki et al. (2007) studied the factors controlling the development of sea-ice over the Sea of Okhotsk. Bond and Adams (2002) and Overland et al. (2002) examined the characteristics of regional air–sea interactions and their relationships to climate patterns over the Bering Sea, respectively. Mysak et al. (1996) and Drinkwater (2004) noted the variability of atmospheric forcing and sea-ice conditions over the Labrador Sea. The climate of the Barents Sea has been studied by Ådlandsvik and

Table 1
The geographic and physical conditions of the sub-arctic seas

	Okhotsk	Bering shelf	Labrador	Barents Sea
Latitude	44–62°N	52–66°N	46–69°N	66–81°N
Longitude	135–160°E	180–150°W	66–43°W	14–66°E
Area of interests (10^6 km^2)	1.47	0.81	2.14	1.49
Average depth (m)	869	65	1773	204
Deepest point	3367	195	4192	479
Shelf area (<200 m) (10^6 km^2)	0.44 (30%)	0.81 (100%)	0.31 (14%)	0.71 (48%)

Area, depth, deepest point and shelf area are calculated from on ETOPO bathymetry data set (Haxby et al., 1983).

Loeng (1991), while Dippner and Ottersen (2001) and Ingvaldsen et al. (2004) showed how climate variations in the Barents Sea are expressed in terms of currents and cod populations.

Here we document the means and fluctuations in the atmospheric forcing of all four regions in a unified manner. The common framework facilitates comparisons between the regions in terms of the mechanisms linking climate forcing to the marine ecosystem.

2. The four basins

The geographic and physical aspects of the four sub-arctic seas are summarized in Table 1; their bathymetries are illustrated in Fig. 1.

The Sea of Okhotsk is a semi-closed sea with an area of 1.5×10^6 km^2. It is located east of the Eurasia continent and bounded by the Kamchatka Peninsula on its eastern side. About one-half of its area is deeper than 1000 m. Narrow passes between the Kuril Islands are conduits for transfer of water between the Sea of Okhotsk and the North Pacific Ocean.

The Bering Sea is located between Eurasia and North America, and contains two distinct regions: the eastern continental shelf and the western deep basin. Its northern boundary includes a narrow Bering Strait, which allows for water exchange with the Arctic Ocean. The southern Bering is bounded by the Alaskan Peninsula and the Aleutian Islands; the passes are relatively shallow (~100–200 m) in eastern portion of the Aleutian Island chain, and are deeper (~1000–3000 m) in its central and western portions (Stabeno et al., 2005). We focus our analysis on the shelf region with an area of 0.8×10^6 km^2, which includes most of the shelf area with the exception of a small portion of the shelf along the Russian coast between 50 and 62.5°N. For simplicity, we refer this region as "Bering Sea shelf". This makes it the smallest of the four sub-arctic regions considered. It is also the most shallow region (typically 30–100 m) of the four.

The Labrador Sea and the Barents Sea represent the Atlantic Ocean counterparts to the Sea of Okhotsk and the Bering Sea. The Labrador Sea is located east of the North America and bounded by Davis Strait to the north and Greenland to the east. Its area is about 2.1×10^6 km^2. It is the deepest on average of the four seas and is also the most open to the larger ocean basins. The Barents Sea is located farther north than the other regions. Its area of 1.5×10^6 km^2 is similar to that of the Sea of Okhotsk. On the north of the Barents Sea two island groups, Franz Josef Land and Svalbard, separate it from the Arctic Ocean.

3. Data sources

Comparative studies require consistency and homogeneity in the data used for analysis. For this reason, our primary source of information was the updated 50+ year-long record of atmospheric variables from the NCEP/NCAR (NN) reanalysis product (Kalnay et al., 1996). The NN reanalysis is produced using a state-of-the-art numerical weather prediction (NWP) model and data assimilation system. Observed data are inserted continually into the model assimilation to constrain the model towards reality; the database used is as complete as possible and it includes both direct and remotely sensed measurements. Our four basins are generally surrounded by quality weather reporting stations, and the NN reanalysis is an excellent method to provide a meteorologically consistent extrapolation into the adjacent oceanic areas.

Table 2
Variables and their corresponding classes in NCEP/NCAR (NN) reanalysis

Variable name	Units	Class
Sea level pressure	hPa	A
Air temperature at 2 m	K	B
Wind component at 10 m	m/s	B
Latent heat flux	W/m^2	C
Sensible heat flux	W/m^2	C
Net short wave radiative flux	W/m^2	C
Net long wave radiative flux	W/m^2	C
Surface wind mixing	$(m/s)^3$	B[a]

See text for explanation of the classes A, B, and C.
[a]This field is derived from the daily surface wind analysis.

The different parameters available from the NN reanalysis vary in the degree to which they are constrained by observations, and to which they are properly accounted for in the NWP model formulation. Therefore the reliability of these parameters has been sorted into three classes (Table 2). In general, the NN reanalysis characterizes the large-scale atmospheric circulation very well; elements of class (A) are strongly influenced by observed data and therefore are most reliable. The next most reliable set of parameters (class B) are also based on direct observations but subject to uncertainties related to model formulations. An example here is provided by the surface wind. Good correspondence has been found between winds from NN reanalysis and independent (unassimilated) measurements from buoys on the Bering Sea shelf (Ladd and Bond, 2002). Parameters that have no direct observations used in the NN reanalysis have relatively greater uncertainty (class C), such as surface sensible and latent heat fluxes, and more highly derived quantities such as radiative heat fluxes. A comparison with in situ data shows that the surface layer meteorological fields are reasonably well represented in the NN reanalysis, but the turbulent heat flux fields contain significant systematic errors (Moore and Renfrew, 2002). To increase the reliability of our estimates we use basin-wide averages. Analysis of interannual to decadal variability on air–sea interaction related fields is based on anomalies, which helps remove the effects of systematic biases. Sea-ice area for each region was calculated from The Met Office Hadley Centre, sea-ice data set (HadISST 1.1). This global sea-ice coverage was constructed based on the combined analysis from variety of sources including digitized sea-ice charts and passive microwave satellite retrievals (http://hadobs.metoffice.com/hadisst/data/download.html). The sea-ice fields are made more homogeneous by compensating satellite microwave-based sea-ice concentrations for the impact of surface melt effects on retrievals and by making the historical in situ concentrations consistent with the satellite data (Rayner et al., 2003).

4. Climatology of the four sub-arctic seas

4.1. Surface air temperature and wind

Surface air temperature (SAT) represents an important aspect of the atmospheric forcing on the ocean, and undergoes large seasonal and longer-term variations in the sub-arctic. Fig. 2 shows the spatial distribution of the SAT over each of the four sub-arctic seas in the four seasons, along with mean wind vectors. The Barents Sea is colder than the other three seas, especially in the transition seasons of May and October, primarily because of its higher latitude. The Labrador Sea has the largest temperature gradients among the four seas, except for summer, when Barents Sea has largest north–south temperature gradient due to the presence of permanent sea ice immediately to its north. During winter the northern part of the Labrador and Barents Seas have average SAT as low as $-30\,^{\circ}C$. The mean SAT isotherms from spring through fall are roughly perpendicular to the winds, implying downstream modification of the atmospheric boundary layer by the relatively warm underlying surface. Three out of four regions have similar, rather uniform distributions of mean SAT in summer (left three panels, third row of Fig. 2), whereas Barents Sea features a significant north–south temperature gradient.

The mean surface winds exhibit systematic changes in direction and magnitude from season to season. Winter (top panels of Fig. 2) is characterized by persistent and relatively strong northerly flow over the Sea of Okhotsk, the Bering Sea shelf, the northern Labrador Seas, and western part of the Barents Sea (wind direction is the direction from which the wind is blowing). A cyclonic (counter clockwise) circulation is indicated over the Barents Sea in association with an extension of the Icelandic Low pressure system. The southerly flow over southeast Barents Sea is a unique feature among the four, and thus explains its relatively warm winter temperatures even at

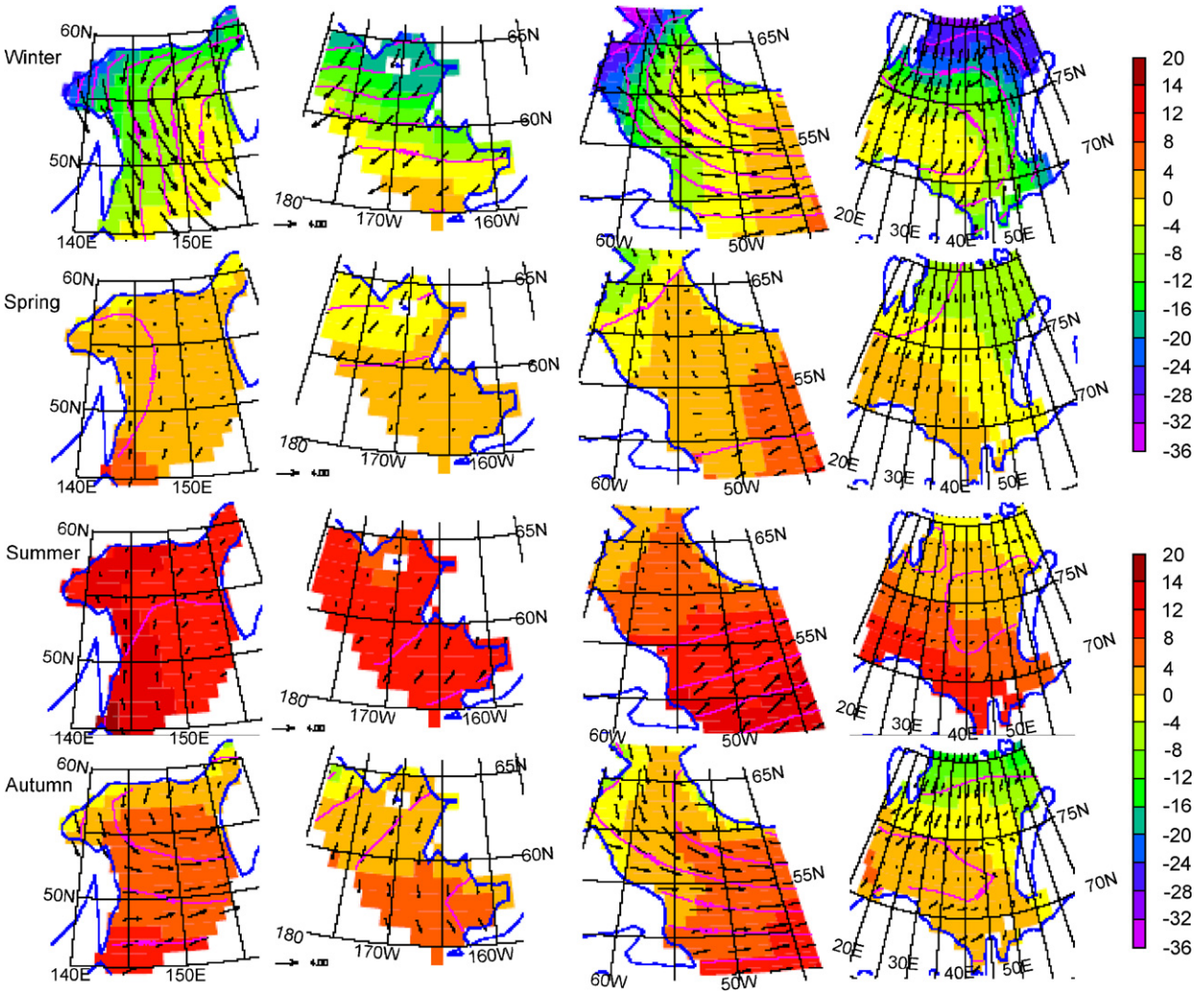

Fig. 2. The climatology of surface air-temperature (shaded), sea-level pressure (SLP) (contour) and surface wind (vectors) for selected month over each of the sub-arctic seas. The climatology is defined as the 50-year (1951–2000) mean based on NN reanalysis. Contour interval is 2 hPa for SLP. From left to right it is for the Sea of Okhotsk, the Bering Sea shelf, the Labrador Sea, and the Barents Sea. From top down, it is for Winter (January), Spring (May), Summer (August), and Autumn (October). The shaded area also indicates the mask of each sub-arctic sea used in area-weighted averages.

latitudes 10–15° farther north than the other seas. Spring features weaker northerly winds, especially in the Sea of Okhotsk. Relatively uniform northerly winds occur in spring in the Barents Sea (right panel of second row of Fig. 2). In summer, mean winds tend to be light, with prevailing southerlies or southwesterlies in their southern parts (third row of Fig. 2). By fall, wind patterns resemble those of winter, especially in the northern portions of the four seas (bottom panels of Fig. 2).

The annual cycle of area-weighted averages of SAT is shown in Fig. 3, which displays similar structure among the four sub-arctic seas. That is, they all have maximum temperature in August and minimum temperature in February. The Barents Sea (dash–dotted line) is the coldest of the four seas throughout the year, and has the smallest variations in the temperature range. The Sea of Okhotsk (solid line) is the warmest region from spring through fall, and also undergoes the largest seasonal variation. The similar seasonal variations among the four indicate a close connection of the four sub-arctic seas in association with the change of the hemispheric general atmospheric circulations.

4.2. Sea-level pressure (SLP)

Spatial distributions of SLP are an indicator of the low-level atmospheric circulation, and are used to diagnose atmospheric variability on seasonal to decadal time scales. Mean SLP maps for the northern hemisphere for winter (December–March) and summer (June–August) are shown in Fig. 4. In winter (left panel), the mean SLP distribution features two low centers, the Aleutian Low over the North Pacific and the Icelandic Low over the North Atlantic, and high pressures over continents with a prominent center over Siberia. The Sea of Okhotsk is located midway between the Aleutian Low and the Siberian High, and the Bering Sea is at the northern periphery of the Aleutian Low. The Labrador Sea and Barents Sea are at the northwest periphery and eastward extension of the Icelandic Low. The summer pattern in mean SLP shows a reversed spatial distribution compared to its winter counterpart, with high pressure centers over the oceans and low pressure centers over the land. But the mean gradients in SLP north of 60°N tend to be weaker in summer than in winter.

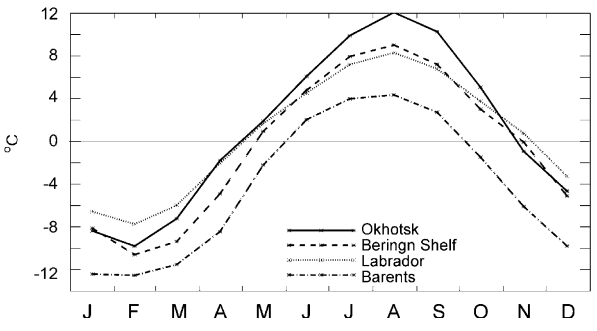

Fig. 3. The seasonal cycles of surface air temperature (SAT) averaged over each sub-arctic sea based on NN reanalysis. The masks shown in Fig. 2, were applied to all the area-weighted averages through the manuscript. Solid line is for averages over the Sea of Okhotsk, dashed line for the Bering Sea Shelf, dotted line for the Labrador Sea and dash–dotted line for the Barents Sea.

The seasonal cycle in large-scale atmospheric forcing based on area-weighted averages of SLP in the Atlantic sector (Fig. 5) is similar between the Labrador Sea (dotted line) and the Barents Sea (dash–dotted line), indicating that both are under the influence of the strength of Icelandic Low. In contrast, the seasonal cycle in area-weighted SLP is rather different between the Sea of Okhotsk (solid) and Bering Sea shelf (dashed) in the Pacific sector. The small magnitude in the seasonal cycle of the area-weighted average of SLP over the Okhotsk Sea (solid) indicates compensation between changes in the strength and location of the Aleutian low and Siberian High over eastern Russia. The seasonal variation of SLP over Bering Shelf shares some similarity with its Atlantic counterpart in the magnitude of variations, but with different timing.

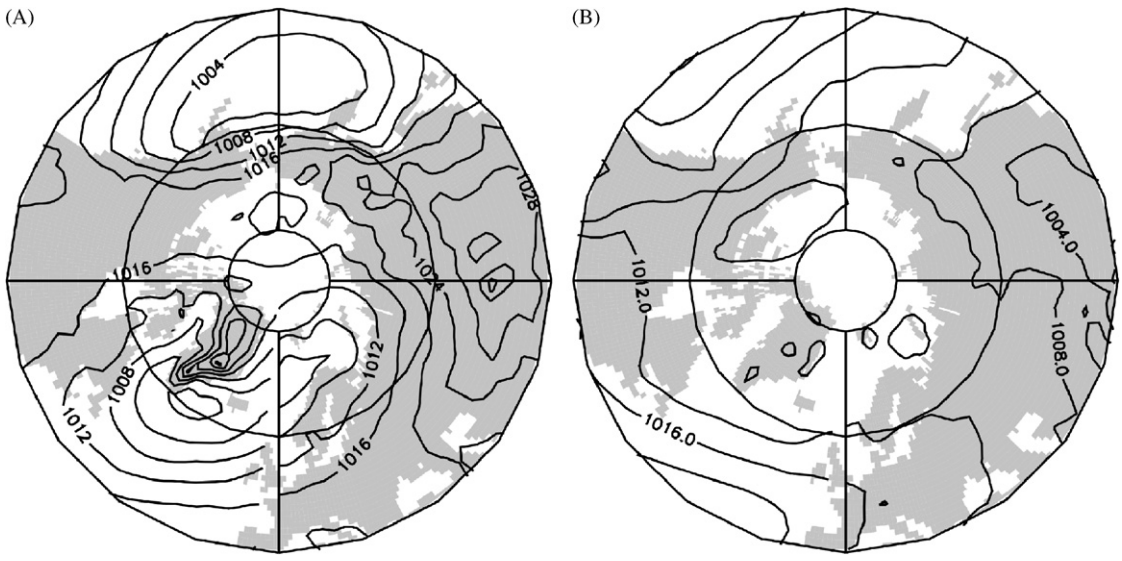

Fig. 4. Seasonal averaged sea level pressure pattern for: (A) winter (DJFM) and (B) summer (JJA) based on 50 year (1951–2000) mean from NN reanalyis. Contour interval is 4 hPa based NN reanalysis.

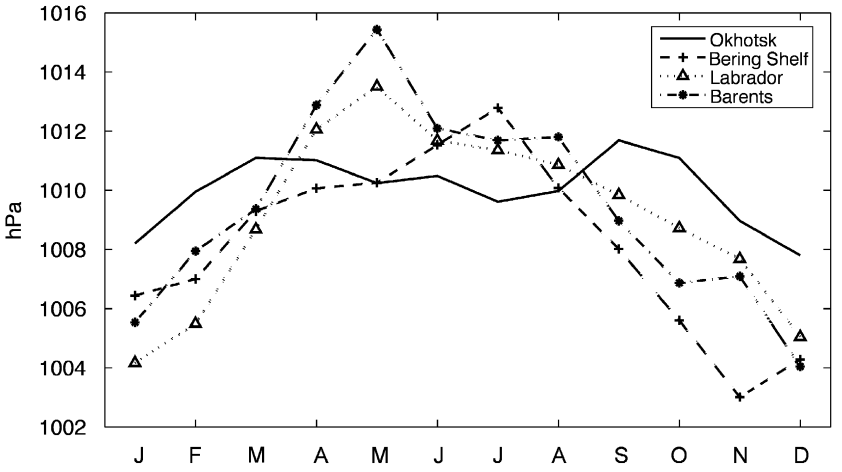

Fig. 5. Seasonal cycle of the area-weighted averages of sea level pressure over the four sub-arctic seas. The climatology is defined as the 50 year (1951–2000) mean based on NN reanalysis.

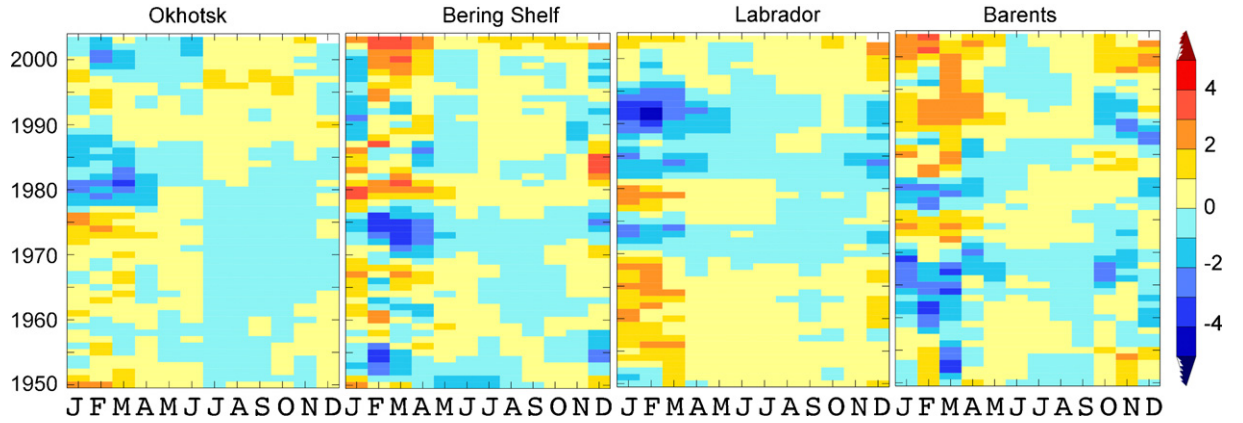

Fig. 6. Monthly (along the *X*-axis) surface air-temperature anomaly averaged over the four sub-arctic seas relative to their 50-year means based on NN reanalysis. The units are in °C. A 3-point running mean was applied on monthly time series before a 5-year running mean applied to annual time series. The *Y*-axis indicates the year.

5. Temporal variability in climate forcing

The objective of this section is to compare variations in the climate forcing of the four sub-arctic seas over the last 56 years (1950–2005), with an emphasis on the similarities and differences among the regions. We begin with fluctuations in air temperature, and show how they relate to concomitant variations in the large-scale atmospheric circulation as represented by changes in SLP.

5.1. Surface air temperature

Monthly SAT anomalies (*X*-axis) in the four regions since 1950 (*Y*-axis) are shown in Fig. 6. All four seas tend to have variations in SAT of greater magnitude in late winter, and of lesser magnitude in late summer. The overall impression is that the four seas have experienced decidedly different fluctuations within and between the seasons over the last 56 years.

The Sea of Okhotsk was relatively warm (cool) from 1950 through the late 1970s during the first (last) half of the year and relatively cool in the last half of the year. The winters turned quite cold in the late 1970s and have mostly remained that way until 2005 with a decade of weak warm-anomalies in the 1990s. Summers have been consistently warm since about 1980. Except for the early 1990s when the warm anomalies occurred throughout the year, the Sea of Okhotsk has the temperature anomalies pattern of opposite phase between the first and

second half of the year. The SAT anomalies over the Bering Sea shelf exhibit greater month-to-month and year-to-year variability than those over the Sea of Okhotsk. Noteworthy variations include a marked shift from cold to warm conditions during winter and spring in the late 1970s that have persisted to the present. The SAT anomalies tend to extend further from winter into the warm season than for the other regions. The reasons for this persistence of SAT anomalies for the Labrador Sea are unclear but may be due to the relatively strong wind mixing in the summer for this location (shown later), which acts to preserve SST anomalies formed in winter. An alternative explanation is that the SST of the Labrador Sea and hence the SAT, is impacted to a greater degree by ocean dynamics (e.g., Lu et al., 2006), particularly horizontal advection, with longer inherent time scales than atmospheric processes. The Labrador Sea experienced largely positive temperature anomalies, particularly during winter, from the early 1950s through the 1970s, and cold winters from 1980 through the mid-1990s, with a few years in late 1980 being characterized by positive anomalies. Large negative anomalies in the early 1990s are unique among the four sub-arctic seas. Since 1995, the region has been generally warmer than normal. The SAT variability for the Barents Sea is characterized by relatively large shorter-term (year to year duration) variability. The winters in the Barents Sea were generally quite cold from the mid-1950s through 1970, and have been mostly warm since about 1980, especially during the last few years.

There has been a fairly systematic inverse relationship or "seesaw" patter between wintertime SAT anomalies in the Labrador Sea and the Barents Sea (the two right panels of Fig. 6), except in the last few years. This seesaw is a signature of a prominent mode of climate variability known as the North Atlantic Oscillation (NAO) (Krahmann and Visbeck, 2003). A comparable inverse relationship between SAT anomalies in the Sea of Okhotsk and Bering shelf is lacking early in the record, but has been present since about 1970 (the two left panels of Fig. 6). One important feature in the SAT anomalies is that three out of four seas (the Bering Sea shelf, the Labrador and the Barents Sea) have been warmer than normal for the last decade. For the Sea of Okhotsk, recent positive anomalies are restricted to the later part of the year. The more-or-less ubiquitous warmth of recent years is unprecedented in the Pacific sector based on the record beginning in 1950, but the North Atlantic did have warm conditions on both sides in the 1930s (Overland et al., 2004).

5.2. Sea-level pressure

Variations in area-weighted averages of SLP can be used to characterize variability in climate/air mass for a region. Fig. 7 displays the SLP anomalies for January and April. Winter (January) is the time of maximum variability in the atmospheric general circulation, as illustrated by the large interannual variability in all four sub-arctic seas (left panel). Although three out of four sub-arctic seas display weak downward trends in their winter SLP anomalies, i.e. increased storminess, the timing of the changes are different: for most of the 56-year periods they are out of phase, until after 2000, when the Bering Sea shelf, the Labrador Sea and the Barents Sea all show strong negative anomalies after a few years of weak positive anomalies around the mid-1990s. During winter, SLP tends to be inversely related to SAT for the Bering Sea shelf and the Barents Seas, but the relationship is not strong for the Sea of Okhotsk and the Labrador Sea. The main reasons are that areas of low pressure at high latitudes tend to be comprised of relatively warm air masses of maritime origin, while areas of high pressure tend to include colder air of arctic or continental origin. This mechanism tends to be accentuated in the Bering Sea shelf and the Barents Sea by the southerly (northerly) wind anomalies that accompany negative (positive) SLP anomalies, since both these basins are east of the locations of greatest SLP variability. Because the Sea of Okhotsk and the Labrador Sea are west of these centers of action, the anomalous meridional (north–south) winds accompanying SLP variations tend to have an ameliorating effect. The time series in Fig. 7 are consistent with this concept. Periods of particularly high pressure occurred around 1970 over the Bering Sea shelf and in the late 1960 over the Barents Sea, which were notably cold periods (Fig. 6). Similarly, the low SLP in the Barents Sea in the early 1990s coincided with a series of particularly warm winters. Since 2000, an inreverse relationship between SLP and SAT has been present in all four sub-arctic seas.

Along with the considerable multi-year variability, the mostly negative trends in SLP over the period of record in all regions are of particular interest. This result suggests that part of the

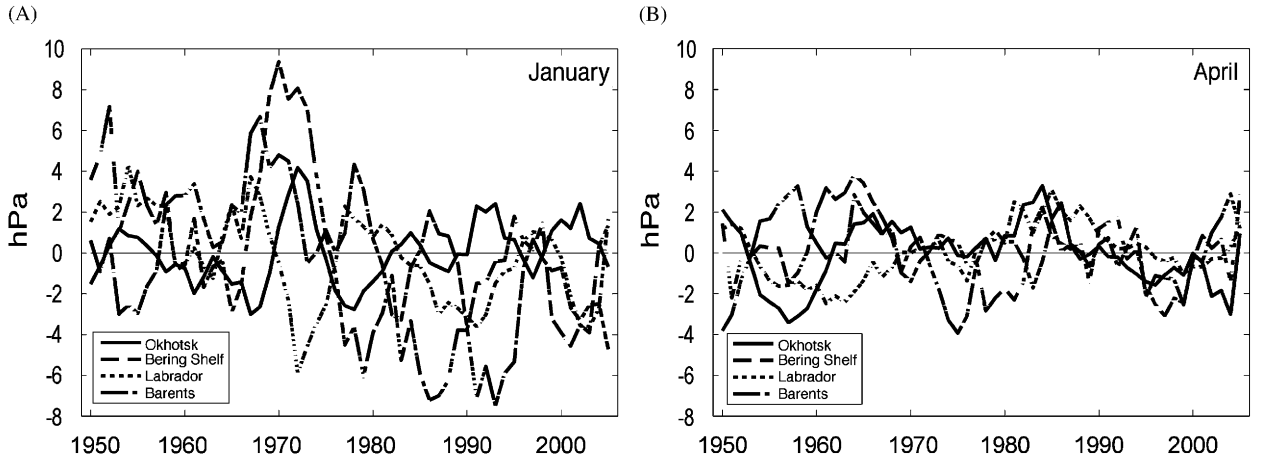

Fig. 7. Area-weighted averages of sea level pressure anomalies over the sub-arctic seas for Winter (January) and Spring (April) relative to the 50-year mean based on NN reanalysis. The units are hPa. A low-pass filter has been applied to the time series. Solid line indicates the Sea of Okhotsk, dashed line indicates the Bering Sea shelf, dotted line indicates the Labrador Sea, and dash-dotted line indicates the Barents Sea.

warming in the sub-arctic regions is a signature of long-term changes in atmospheric circulation, namely a poleward shift in the locations of the Aleutian and Icelandic lows in winter. Spring (April) is a critical season for ecosystem productivity, as its conditions closely relate to the spring bloom and ice retreat; yet the time series of SLP for April include much less temporal variability than their counterparts for January. The inter-decadal variability in these series is relatively small since the mid-1980s, and the SLP has tended to be low in the last 10 years. July (not shown) has small variability in SLP, consistent with radiative processes dominating air–sea interactions in summer.

6. Surface fluxes

6.1. Climatology of surface heat fluxes

Surface fluxes represent the energy exchanges between the ocean and the atmosphere. As mentioned earlier, there is relatively meager direct information on these parameters. The NN reanalysis does provide a complete set of surface fluxes through the parameterizations incorporated in the NWP model used as its foundation. These parameterizations yield errors; however, due to the necessary simplifications inherent to the parameterization schemes, and due to lack of data. For example, net radiation at the surface is 5–8 W/m^2 less from the NN reanalysis in terms of global means compared with climatological estimates (Kalnay et al., 1996). For this reason, we do not emphasize the absolute values of these fields, focusing instead on their seasonal variability and the relative differences among the four sub-arctic seas.

The seasonal cycle of sensible heat, latent heat, net total (short and long wave) radiation, and total net heat fluxes averaged over the four seas are shown in Fig. 8 with positive numbers indicating that the ocean gains energy from the atmosphere (note the different vertical scales in each sub-plot). The seasonal cycles of these fluxes are strikingly similar among the four sub-arctic seas, with only slight differences in magnitude. The change in the seasonal cycle of the solar insolation is mainly caused by the length of the day, the solar inclination angle, and the latitude of the four basins.

In summer (June–August) the sensible-heat fluxes are positive (air to ocean), implying that air temperatures are warmer than the SST for all four sub-arctic seas (Fig. 8A). This is the only period when the ocean gains the energy from the atmosphere. The large magnitudes in the sensible-heat fluxes in winter are associated with the combination of strong winds and cold SATs. The latent-heat flux (Fig. 8B) shows similar seasonal cycles as the sensible heat fluxes, with the maximum transfer from the ocean to the air in October–March. The seasonal cycle of the net radiative fluxes indicates 40–60 W/m^2 of heat loss to the atmosphere in the

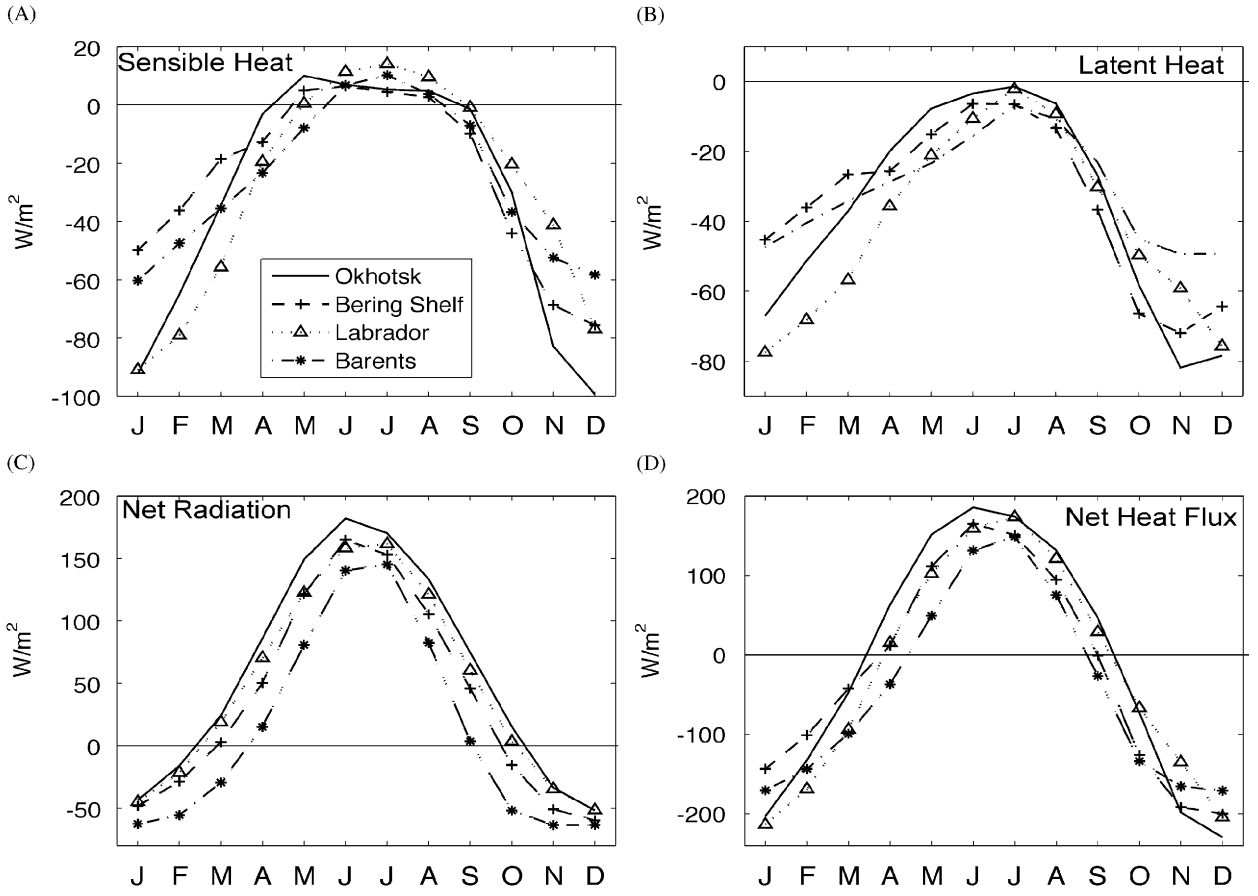

Fig. 8. The seasonal cycle of surface fluxes averaged over each sub-arctic seas based on NN reanalysis. The units are W/m^2, with positive number indicating downward flux, in another words, the ocean gains energy from the atmosphere. Solid line indicates the Sea of Okhotsk, dashed line indicates the Bering Sea shelf, dotted line indicates the Labrador Sea, and dash–dotted line indicates the Barents Sea.

winter (Fig. 8C), when the sun angle is low and days are short, and hence the solar heating is minimal, especially in the Barents Sea. In summer, the heat loss due to the net longwave radiative fluxes is much less than the gain from net shortwave fluxes, which results in a heating of the ocean by as much as $200\,W/m^2$.

The seasonal cycles in the net heat fluxes (Fig. 8D) including sensible heat, latent-heat fluxes and net radiation flux (short and long wave) are similar to the net radiative forcing, but there are some distinctions worth noting. For all four sub-arctic seas, the ocean loses heat to the atmosphere during winter (October–March) and gains heat from the atmosphere in summer. The magnitudes of the seasonal cycles are greater in the Sea of Okhotsk (solid) and Labrador Sea (dotted), which are consistent with the greatest seasonal cycle of SAT those regions experienced. The peak heating in the Sea of Okhotsk and the Bering Sea shelf is in June, while for the Labrador Sea and the Barents Sea it is in July. This difference in phasing is mostly attributable to differences in the net shortwave fluxes, apparently in association with the lingering of sea ice and hence higher albedos, in the Labrador and Barents Seas as will be shown later.

The spatial distributions of the seasonally averaged fluxes (not shown) reveal similar patterns among the four sub-arctic seas: north-south gradients in the fluxes with greater fluxes in the north: out of the ocean in winter and into the ocean in summer. There are significant spatial variations in the mean fluxes in selected regions, in particular within the Labrador Sea.

6.2. *Variation in surface heat fluxes*

The variability in monthly anomalies of the sensible heat, latent heat, net radiation, and the total heat fluxes at the surface, averaged over each

region, are shown in Fig. 9. As discussed earlier, while these fluxes are based on model parameterizations, they are also constrained by observations, and hence represent reasonable estimates, especially in a comparative sense.

On a monthly basis, the anomalies can be as large as 20 W/m^2 for the net heat flux (top panels of Fig. 9). The temporal pattern in the net heat-flux anomalies for the Sea of Okhotsk resembles those for the Bering Sea shelf. Both have had positive anomalies in recent decades during winter and spring, and negative anomalies in summer (to a lesser degree for the Bering Sea shelf). Mostly negative heat-flux anomalies occurred in both seas before 1980. The strongest positive anomalies for the Sea of Okhotsk occur in winter, whereas for the Bering Sea shelf they tend to occur in spring. The positive anomalies in the heat flux indicate a *reduction of heat loss* to the atmosphere, and in turn it would contribute to warm ocean temperature anomalies and reduction of sea-ice cover. This is especially critical in spring when the net heat flux is close to zero. Over the Bering Sea shelf, this result is consistent with the trend towards increased water temperature over the shelf (Overland and Stabeno, 2004) and early ice retreat plus less ice coverage for 2000–2005 (Hunt et al., 2002; Stabeno et al., 2007).

The temporal character of the net heat-flux anomalies was different in the Atlantic sector. In recent decades, the Labrador Sea and the Barents Sea have experienced their positive heat-flux anomalies principally during summer. Strong negative anomalies are observed in winter during the early 1990s over the Labrador Sea and after 2000 over the Barents Sea. Before 1970, the pattern is reversed: there were positive anomalies in winter and negative anomalies in summer for the Labrador Sea. There is large decadal variability in winter net heat-flux anomalies over the Barents Sea.

The variations in individual components of the heat fluxes are discussed below. The decadal variations in the surface sensible heat fluxes (Fig. 9 second row) are more prominent during winter and spring (November–May) than during the warm season (June–October). All regions except the Barents Sea experienced positive anomalies in recent decades, with the strongest signal in the Sea of Okhotsk. In general, the magnitudes of anomalies over the Bering Sea shelf and the Barents Sea are weak compared with their counterparts for the Sea of Okhotsk and the Labrador Sea in winter. The negative relationship between SAT and sensible heat-flux anomalies in the Sea of Okhotsk is related to its large variations in sea-ice coverage. Sea ice effectively suppresses the sensible heat lost by the ocean to the atmosphere in winter; this effect has been more pronounced during the 1980s because of relatively heavy sea ice. A confounding factor is oceanic heat content changes associated with the freezing and melting of sea ice (shown later in Section 7). These phase changes occur not just at different times but generally in different locations and hence complicate heat budgets. The co-variability between the sensible heat flux and SAT anomalies is not as apparent during the warm season, which is not surprising since the magnitudes of both tend to be weak.

The variations in latent heat flux anomalies (third row of Fig. 9) are relatively weak in magnitude, but otherwise resemble their sensible heat flux counterparts. This correspondence means that the atmosphere tends to be relatively moist (dry) when it is warm (cold) on interannual time scales. One noteworthy difference between the Pacific and Atlantic regions is that in the last 15–20 years, the sensible- and latent-heat fluxes have caused anomalous heating of the Sea of Okhotsk and the Bering Sea shelf, and anomalous cooling of the Barents Sea, principally during winter and spring.

The net radiative flux anomalies were positive recently for all four seas, with some differences in seasonality. The radiative heating anomalies have been concentrated in the spring in the Sea of Okhotsk and Bering Sea shelf, and more during late spring through summer for the Labrador and the Barents Seas due to reduced cloud cover (not shown). The anomaly patterns are persistent from month to month for the Labrador Sea. For the remaining three seas, the anomaly pattern is more persistent from year-to-year, with opposite sign of changes between seasons. This is especially true for the Barents Sea, where winter and summer anomalies are often of opposite sign.

With regards to the individual components of the net heat fluxes, the sensible- and latent-heat flux components dominate the variability in the Sea of Okhotsk and the Labrador Sea, while all three components of the net fluxes play comparable roles over the Bering Sea shelf. For the Barents Sea, the net radiative fluxes are most important in summer, whereas in winter all three components have anomalies of comparable magnitude. The dominance of the sensible- and latent-heat fluxes in the Sea of Okhotsk and the Labrador Sea reflect the

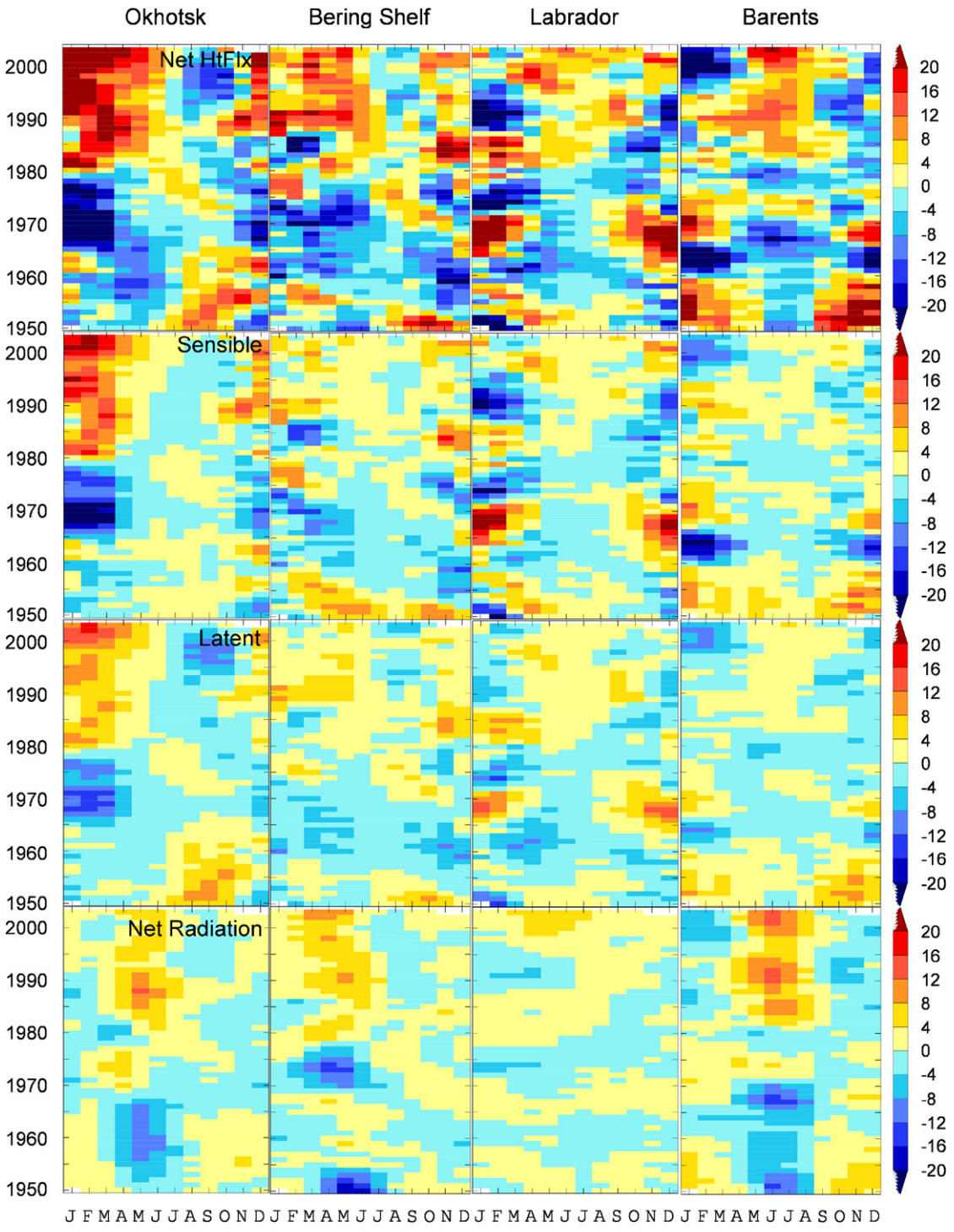

Fig. 9. Monthly surface heat flux anomalies averaged over the four sub-arctic seas based on NN reanalysis. From top down it is for net heat fluxes, sensible heat, latent heat, and net radiative flux. The units are in W/m^2, and positive numbers (warm colors) indicating downward fluxes. From left to right the panels are for the Sea of Okhotsk, the Bering Sea shelf, the Labrador Sea and the Barents Sea. A 3-point running mean was applied on monthly time series before a 5-year running mean applied to the annual time series for each individual month.

prevalence of cold, dry air masses of continental origin relative to the Bering Sea shelf and the Barents Sea.

While there have been periods of significantly negative net heat-flux anomalies in the last two decades in all four regions, these anomalies have lacked persistence from season to season. There tended to be less seasonality to the net cooling events before the 1980s. While our analysis precludes differentiating cause from effect, previous work indicates that it is the atmosphere that largely controls the variability in air–sea interactions over the North Pacific and North Atlantic (Kushnir et al., 2002).

6.3. Climatology and variations of wind mixing

The energy available for mechanical mixing of the ocean is approximately proportional to the cube of the wind speed. Therefore, episodic storms have particularly large impacts on ocean stratification and vertical exchanges. Wind-induced mixing is particularly important in summer because it can increase nutrient concentrations in the upper part of the water column and hence sustain primary productivity beyond the spring bloom (e.g., Sambroto et al., 1986). As shown in Fig. 10, the spatial pattern of wind mixing is quite similar between winter (top) and summer (bottom). During warm months (May–September) mixing over the four sub-arctic seas is about one-fourth to one-third of its winter magnitude. The mixing is quite strong in the middle of the Labrador Sea in winter (Fig. 10, third panel, top row). A similar pattern is also seen over the Sea of Okhotsk (Fig. 10, left panel, top row). The magnitudes of the mixing for the other two seas are much weaker in winter. The mixing in Sea of the Okhotsk is stronger in winter than the two shallow seas, the Bering Sea shelf and the Barents Sea, in part because of the persistently strong north winds in association with the Siberian High to the west and the Aleutian low to the east. On the other hand, the Sea of Okhotsk has the weakest wind mixing among the four seas in summer, due to a much reduced mean SLP gradient.

The time series of wind-mixing anomalies for a selected location in each sea are shown in Fig. 11. These time series, constructed from daily wind analyses, better characterize the true nature of the variability in wind mixing as monthly, basin-averages smooth out the effects of smaller scale meteorological features such as fronts and cyclonic storms. Strong interannual variability of mixing occurs in all four sub-arctic seas throughout the year due to the highly episodic aspect of this component of atmospheric forcing. Winter (November–March) obviously has larger amplitude anomalies than the other seasons. There has been reduced winter wind mixing in the center of the Sea of Okhotsk (52°N, 148°E) since late 1970s. Reduced mixing in late winter near St. Paul Island (57.5°N, 170°W) on the Bering Sea shelf since 1996, and over

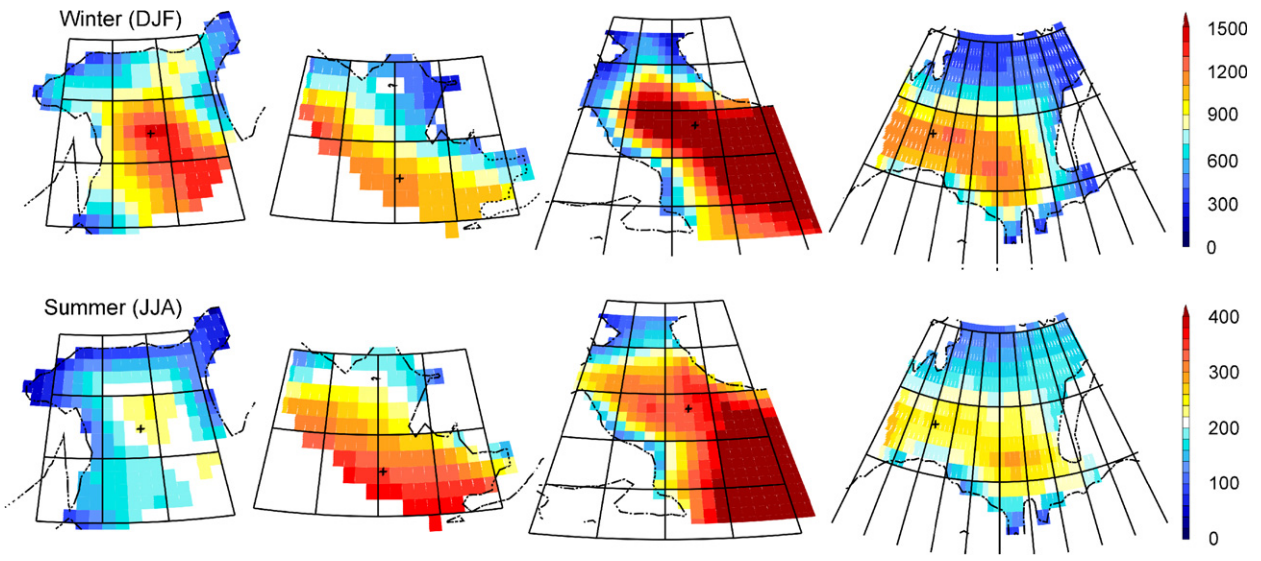

Fig. 10. Winter (DJF) and summer (JJA) wind mixing pattern for each sub-arctic sea in units of $(m/s)^3$ based on NN reanalysis. The "+" in each plot indicates the location of the anomalies to be presented in Fig. 11.

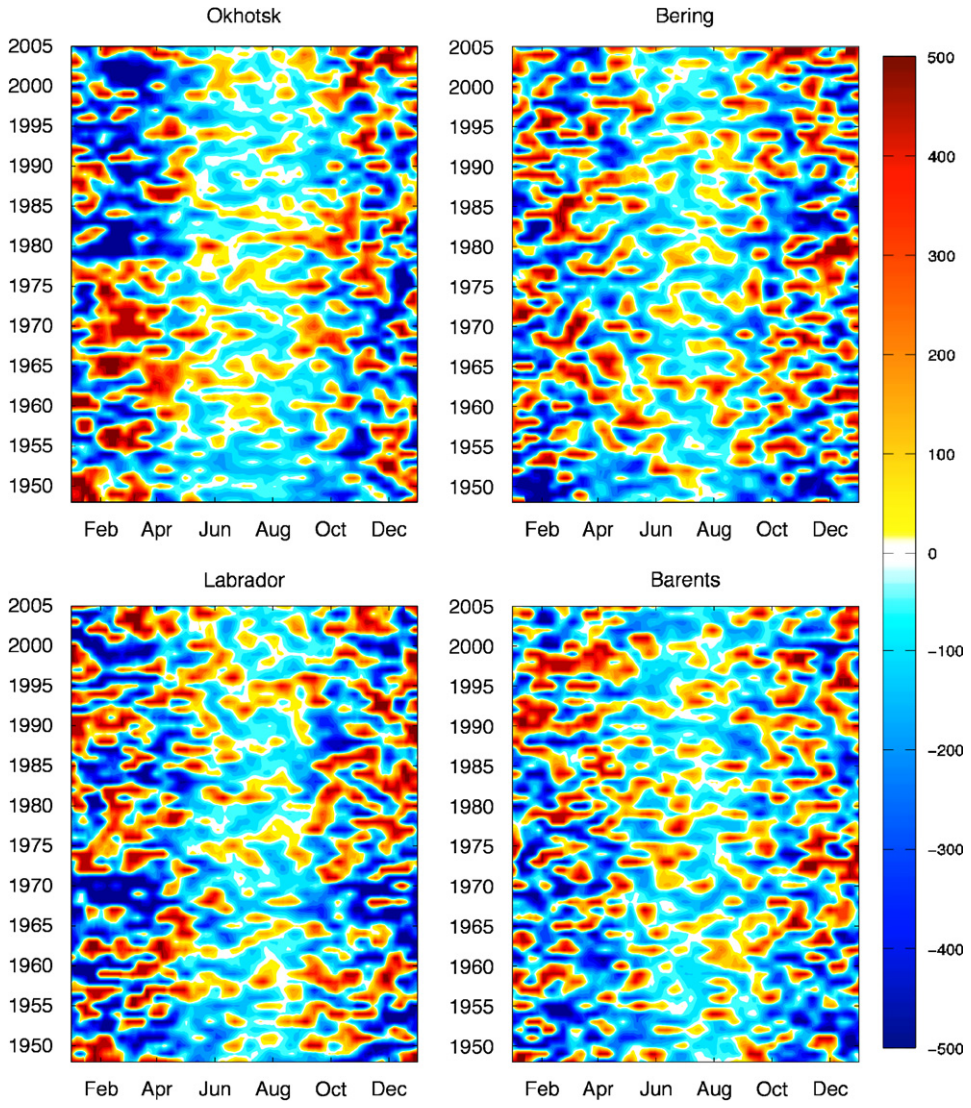

Fig. 11. Daily wind mixing anomaly (wind speed cubed) at selected point in each region for 1948–2005, smoothed by a low-pass filter based on NN reanalysis. Units are $(m/s)^3$.

the southwest Barents Sea (73°N, 25°E) since 2000 are also evident; however, the magnitude of change is not as strong as that over the Sea of Okhotsk. In the center of the Labrador Sea (55°N, 53°W), increased mixing has occurred in most of the winters since 1970.

7. Sea ice conditions: means and variability

A common feature among the four sub-arctic seas is their seasonal ice cover. Fig. 12 shows the seasonal cycle of the ice area for each of them based on the analysis from HadISST (Rayner et al., 2003). Due to the permanent ice cover in its northern boundary adjacent to the central Arctic Ocean, the Barents Sea is the only one of the four with ice coverage in the summer. Ice-free conditions begin earlier and last longer for the Pacific sectors than for the Atlantic counterparts. In spring, the rate of ice area decrease is the fastest in the Sea of Okhotsk (solid line). Ice retreat stars a month later in May in the Barents Sea mainly due to its higher latitude location. In the fall, the growth of sea ice is fastest in the Barents Sea. By November, when the other three sub-arctic seas are just starting to accumulate sea-ice coverage, the sea-ice area in Barents Sea is already close to 50% of its maximum value.

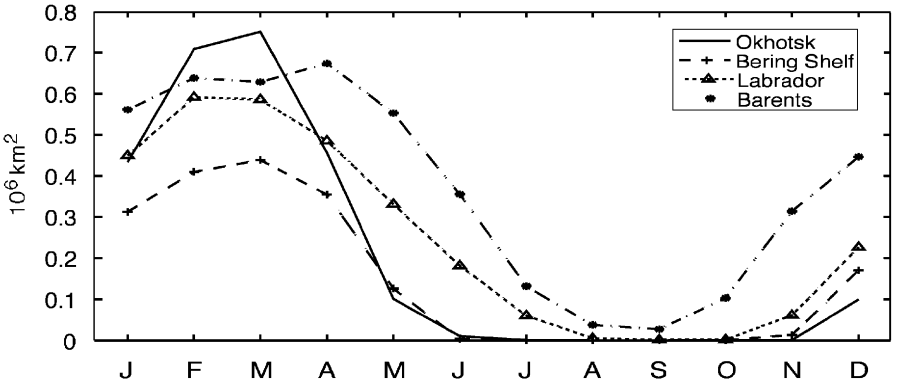

Fig. 12. Seasonal cycle of ice area over the sub-arctic seas. Units are 10^6 km^2 based on HadISST monthly sea-ice concentration analysis.

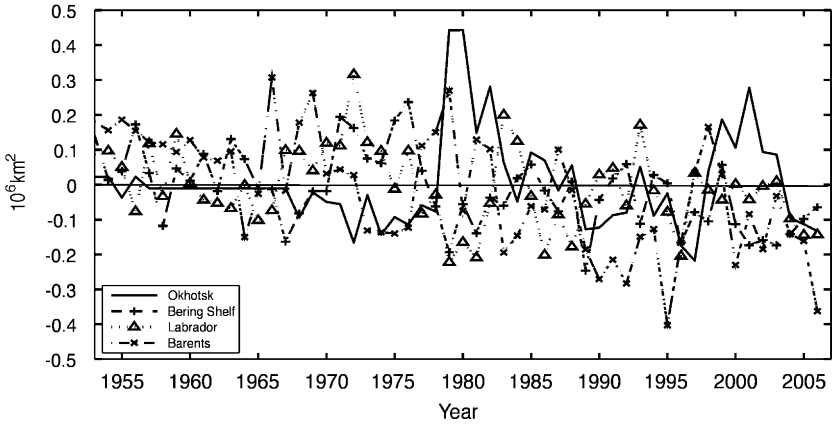

Fig. 13. Ice-area anomaly for spring (March and April average) relative to 1953–2000 mean for the four sub-arctic seas based on HadISST monthly sea-ice concentration analysis. Units are 10^6 km^2. The data before 1979 were based on ship observations, so the density and frequency were not evenly distributed. It is more reliable after 1979 with blending in the satellite observations.

Even though the sea-ice data time series exists as far back as the 1870s, the quality of the data is more reliable after 1953 simply because the earlier observations were sparse. Thus, for consistency with our other plots, the sea-ice area anomalies are shown from 1953 in Fig. 13. Even so, caution must be used in interpretation of the sea-ice data. For example, the sudden jump in the sea-ice area from 1978 to 1979 over Sea of Okhotsk (solid line of Fig. 13) must be due to the introduction of satellite data into the analysis. This is not a significant problem in other regions, however, presumably due to better coverage from ship data. Large interannual variability is seen in the ice-area for each of the basins. Even though there is no significant linear trend in the time series for the past 56 years as a whole, negative ice-area anomalies since the late 1990s are apparent for all but the Sea of Okhotsk. This finding is consistent with the positive temperature anomalies shown in Fig. 6 and the positive net heat fluxes into the ocean in spring over recent decades shown in Fig. 9. The reduced ice coverage over the Bering Sea shelf in recent years also was reported by Hunt et al. (2002) and Stabeno et al. (2007). Not only is there less ice coverage over southeast Bering Sea shelf, but the ice has recently been retreating earlier in spring.

8. Final remarks

A 56-year record from the NN reanalysis plus the sea-ice analysis from The Met Office Hadley Centre have been used to document air–sea interactions in the four sub-arctic seas. The mean seasonal cycles in SAT and heat fluxes are comparable in the four regions. There are larger meridional temperature gradients and seasonal cycles in the winds for the Sea of Okhotsk and the Labrador Sea than for their

counterparts to the east, the Bering Sea shelf and the Barents Seas. We expect that the prominent seasonal cycles in the winds for the Sea of Okhotsk and the Labrador Sea may force a significant seasonal cycle in currents along the western coasts of each of these basins (e.g., Thompson et al., 1986 with regards to the Labrador Sea), with implications for transports and ocean ventilation. The enhanced seasonal cycle in SAT (which itself is tightly coupled to the SST) in the Labrador Sea suggests relatively large warm-season thermal stratification.

The four sub-arctic seas have experienced different timing in their anomalous climate forcing. Air–sea interactions in all four regions have undergone complicated patterns of temporal variability, but with the common thread of major warm temperature anomalies and less ice coverage in spring in recent years. Although three out of four sub-arctic seas display downward trends in their winter SLP anomalies, coherence between their interannual to decadal variations is lacking. Regarding SAT anomalies, our analysis reproduces the well-known seesaw pattern between the Labrador and Barents Sea over the Atlantic sector, which is a signature of NAO (e.g., Krahmann and Visbeck, 2003). Over the Pacific sector, the co-variability between the Sea of Okhotsk and the Being Sea shelf is only evident in recent decades. The Sea of Okhotsk displays systematic changes around the late 1970s, and shows opposite sign of change for the first and second half of the year; this reflects the influence of variability in the Siberian high, which has a weaker counterpart in North America (as illustrated in Fig. 4). The net heat-flux anomalies have switched from negative to positive for the Sea of Okhotsk and the Bering Sea shelf during the winter and spring in the last two decades. The net heating in spring appears to be especially important on the Bering Sea shelf. The mean net heat fluxes in April are $\sim 10\,W/m^2$ and hence modest heat-flux anomalies have large impacts on the melting/retreat of sea ice. The Labrador and Barents Seas have experienced different decadal variations in net heating than their Pacific counterparts; the positive heat-flux anomalies in the Atlantic regions have occurred generally in summer, principally due to anomalous radiative heating.

Much of the previous work on climate–ecosystem linkages has used large-scale indices such as the NAO and Pacific Decadal Oscillation to characterize the climate variability (e.g. Hurrell and van Loon, 1997; Mantua et al., 1997). This approach does not account for the actual mechanisms involved in the ocean's response to climate forcing. Thus we recommend a closer look at the local air–sea interatction parameters that affect ocean productivity, and only then relate these parameters to hemispheric climate variability. At the very least, our results show that there is a high degree of seasonality in the nature and sense of the air–sea interactions, which we feel has not yet been sufficiently appreciated. Our primary objective has been to document these variations and thereby provide the context for further comparative studies of climate-marine ecosystem linkages in sub-arctic seas.

Acknowledgments

Preparation of this manuscript was supported by the National Oceanic and Atmospheric Administrations (NOAA) Arctic Research Program and the NOAA Fisheries–Oceanography Coordinated Investigations (FOCI) program. We thank George Hunt for his thorough reading and extensive editing on the manuscript, and helpful suggestions. This publication was partially completed through the Joint Institute for the Study of the Atmosphere and Ocean (JISAO) under NOAA Cooperative Agreement no. NA17RJ1232, Contribution no 1314. The Pacific Marine Environmental Laboratory Contribution no # 2926, and is contribution EcoFOCI-0683 to FOCI program. This paper was first presented in the GLOBEC-ESSAS Symposium on "Effects of climate variability on sub-artic marine ecosystems", hosted by PICES in Victoria, BC, May 2005.

References

Ådlandsvik, B., Loeng, H., 1991. A study of the climate system in the Barents Sea. Polar Research 10, 45–49.

Baier, C.T., Napp, J.M., 2003. Climate-induced variability in Calanus marshallae populations. Journal of Plankton Research 25, 771–782.

Bond, N.A., Adams, J.M., 2002. Atmospheric forcing of the southeast Bering Sea in 1995–1999 in the context of a 40 year historical record. Deep-Sea Research II 49, 5869–5887.

Dippner, J.W., Ottersen, G., 2001. Cod and climate variability in the Barents Sea. Climate Research 17, 73–82.

Drinkwater, K.F., 2002. A review of the role of climate variability in the decline of northern cod. American Fisheries Society Symposium 32, 113–130.

Drinkwater, K., 2004. Atmospheric and sea-ice conditions in the northwest Atlantic during the decade 1991–2000. Journal of Northwest Atlantic Fishery Science 34, 1–11.

Haxby, W.F., Labrecque, J.L., Weissel, J.K., Karner, G.D., 1983. Digital images of combined oceanic and continental data sets and their use in tectonic studies. EOS Transactions of the American Physical Union 64 (52), 995–1004.

Hunt Jr., G.L., Drinkwater, K. (Eds.), 2005. Background on the climatology, physical oceanography and ecosystems of the sub-arctic seas: Appendix to the ESSAS Science Plan. GLOBEC Report No. 20, viii, 96pp.

Hunt Jr., G.L., Stabeno, P., Walters, G., Sinclair, E., Brodeur, R.D., Napp, J.M., Bond, N.A., 2002. Climate change and control of the southeastern Bering Sea pelagic ecosystem. Deep-Sea Research II 49, 5821–5853.

Hunt Jr., G.L., Megrey, B.A., 2005. Comparison of the biophysical and trophic characteristics of the Bering and Barents Seas. ICES Journal of Marine Science 62, 1245–1255.

Hurrell, J.W., van Loon, H., 1997. Decadal variations in climate associated with the North Atlantic oscillation. Climatic Change 36, 301–326.

Ingvaldsen, R., Asplin, L., Loeng, H., 2004. The seasonal cycle in the Atlantic transport to the Barents Sea during the years 1997–2001. Continental Shelf Research 24, 1015–1032.

Kalnay, E., Kanamitsu, M., Kistler, R., Collins, W., Deaven, D., Gandin, L., Iredell, M., Saha, S., White, G., Woollen, J., Zhu, Y., Chelliah, M., Ebisuzaki, W., Higgins, W., Janowiak, J., Mo, K.C., Ropelewski, C., Wang, J., Leetmaa, A., Reynolds, R., Jenne, R., Joseph, D., 1996. The NCEP/NCAR 40-year reanalysis project. Bulletin of the American Meteorological Society 77, 437–471.

Krahmann, G., Visbeck, M., 2003. Variability in Northern Annular Mode's signature in winter sea Ice concentration. Polar Research 21, 51–57.

Kushnir, Y., Robinson, W.A., Blade, I., Hall, N.M.J., Peng, S., Sutton, R., 2002. Atmospheric GCM response to extratropical SST anomalies: synthesis and evaluation. Journal of Climate 15, 2233–2256.

Ladd, C., Bond, N.A., 2002. Evaluation of the NCEP-NCAR Reanalysis in the northeast Pacific and the Bering Sea. Journal of Geophysical Research 107, 3158.

Liu, J.P., Zhang, Z., Horton, R.M., Wang, C., Ren, X., 2007. Variability of North Pacific sea ice and East Asia-North Pacific winter climate. Journal of Climate 20, 1991–2001.

Lu, Y., Wright, D.G., Clarke, R.A., 2006. Modelling deep seasonal temperature changes in the Labrador Sea. Geophysics Research Letter 33, L23601.

Mantua, N.J., Hare, S.R., Zhang, Y., Wallace, J.M., Francis, R.C., 1997. A Pacific interdecadal climate oscillation with impacts on salmon production. Bulletin of the American Meteorological Society 78, 1069–1079.

Moore, G.W.K., Renfrew, I.A., 2002. An assessment of the surface turbulent heat fluxes from the NCEP reanalysis over the western boundary currents. Journal of Climate 15, 2020–2037.

Mysak, L.A., Ingram, R.G., Wang, J., van der Baaren, A., 1996. Anomalous sea-ice extent in Hudson Bay, Baffin Bay and the Labrador Sea during three simultaneous ENSO and NAO episodes. Atmosphere—Ocean 34, 313–343.

Ottersen, G., Aadlandsvik, B., Loeng, H., 2000. Prediction of temperature in the Barents Sea. Fisheries Oceanography 9, 121–135.

Ottersen, G., Alheit, J., Drinkwater, K., Friedland, K., Hagen, E., Stenseth, N.C., 2004. The response of fish to ocean climate variability. In: Stenseth, N.C., Ottersen, G., Hurrell, J., Belgrano, A. (Eds.), Marine Ecosystems and Climate Variation: the North Atlantic. Oxford University Press, Oxford, UK, pp. 71–94.

Overland, J.E., Stabeno, P.J., 2004. Is the climate of the Bering Sea warming and affecting the ecosystem? EOS, Transactions of the American Geophysical Union 85, 309–312.

Overland, J.E., Bond, N.A., Adams, J.M., 2002. The relation of surface forcing of the Bering Sea to large-scale climate patterns. Deep-Sea Research II 49, 5855–5868.

Overland, J.E., Spillane, M.C., Percival, D.B., Wang, M., Mofjeld, H.O., 2004. Seasonal and regional variation of Pan-Arctic air temperature over the instrumental record. Journal of Climate 17, 3263–3282.

Rayner, N.A., Parker, E., Horton, E.B., Folland, C.K., Alexander, L.V., Rowell, D.P., Kent, E.C., Kaplan, A., 2003. Global analyses of sea surface temperature, sea ice, and night marine air temperature since the late nineteenth century. Journal of Geophysical Research 108, 4407.

Sambroto, R.N., Niebauer, H.J., Goering, J.J., Iverson, R.L., 1986. Relationships among vertical mixing, nitrate uptake and phytoplankton growth during the spring bloom in the southeast Bering Sea middle shelf. Continental Shelf Research 5, 161–198.

Sasaki, Y.N., Katagiri, Y., Minobe, S., Rigor, I.G., 2007. Autumn atmospheric preconditioning for interannual variability of wintertime sea-ice in the Okhotsk Sea. Journal of Oceanograph 63, 255–265.

Stabeno, P.J., Kachel, D.G., Kachel, N.B., Sullivan, M.E., 2005. Observations from moorings in the Aleutian Passes: temperature, salinity and transport. Fisheries Oceanography 14 (Supplement 1), 39–54.

Stabeno, P.J., Bond, N.A., Salo, S.A., 2007. On the recent warming of the southeastern Bering Sea Shelf. Progress in Oceanography [in press].

Thompson, K.R., Lazier, J.N.R., Taylor, B., 1986. Wind-forced changes in Labrador Current transport. Journal of Geophysical Research 91, 14261–14268.